

Dynamic scaling in rotating turbulence: A shell model studyShailendra K. Rathor^{1,*}, Sagar Chakraborty^{1,†} and Samriddhi Sankar Ray^{2,‡}¹*Department of Physics, Indian Institute of Technology Kanpur, Uttar Pradesh 208016, India*²*International Centre for Theoretical Sciences, Tata Institute of Fundamental Research, Bangalore 560089, India*

(Received 23 December 2021; accepted 16 May 2022; published 10 June 2022)

We investigate the scaling form of appropriate timescales extracted from time-dependent correlation functions in rotating turbulent flows. In particular, we obtain precise estimates of the dynamic exponents z_p , associated with the timescales, and their relation with the more commonly measured equal-time exponents ζ_p . These theoretical predictions, obtained by using the multifractal formalism, are validated through extensive numerical simulations of a shell model for such rotating flows.

DOI: [10.1103/PhysRevE.105.L063102](https://doi.org/10.1103/PhysRevE.105.L063102)

Many aspects of turbulence are understood through p th-order correlation functions of velocity increments across suitably defined length scales r which lie in the so-called inertial ranges of the flow [1–3]. In simple terms, the inertial range is well separated from and lies between the system-dependent energy injection scale L and dissipation scale η of the turbulent flow. We now know that there exist power laws [3–5] in these correlators, typically called structure functions, and a universality of the associated scaling exponents ζ_p which are perhaps universal for a given class of turbulent flows but may well vary for different forms of turbulence. Thus, the evidence favoring the universality of such exponents in fully developed, homogeneous and isotropic [3,6,7], passive-scalar [6,8–10], magnetohydrodynamic [11–13], two-dimensional [14–17], and indeed rotating turbulence [18–21], to name a few, is overwhelming. Nevertheless, the values of ζ_p are known to be different and specific to each of these turbulent flows.

The algebraic nature of these structure functions and indeed the universality of the exponents also are reminiscent of the behavior of correlation functions near a critical point [22], for example, in spin systems. However, for the turbulent flows that we are familiar with this analogy is limited [23]. This is because in fully developed turbulence an infinite set of exponents is required to fully characterize different-order structure functions in the inertial range as opposed to the simple scaling one is familiar with in critical phenomena. Such a complexity, which can be rationalized through a multifractal description of turbulent flows, has also meant that, unlike in critical phenomena where studies of static and dynamic correlators [24] have been closely associated, the study of time-dependent structure functions is more recent in turbulence.

Nevertheless, over the past decades there has been a concerted effort to generalize the dynamic-scaling ansatz in the critical phenomenon, namely, the dynamic scaling exponent z associated with the relaxation time τ near a critical point, and

obtain estimates of the multiscale nature of time-dependent structure functions in turbulence. These investigations have however been limited to homogeneous, isotropic turbulence in two and three dimensions or for the case of passive-scalar turbulence [16,25–29]. In particular, these studies demonstrate that just like the case of equal-time exponents ζ_p , there exists an infinite set of (universal) exponents z_p whose values depend on the kind of relaxation time taken from the order- p time-dependent structure functions. Perhaps the most important success of these studies was the generalization of the Frisch-Parisi multifractal formalism [30] for the velocity field \mathbf{u} to derive (linear) bridge relations [26,31,32] connecting the dynamic z_p and equal-time ζ_p exponents and to establish the notion of dynamic multiscaling.

The complex nature of time correlations in these systems is intrinsic. However, what happens when there is an external global timescale governing the statistical nature of the turbulent flow itself? Indeed, for such systems it is difficult to separate the hierarchy of dynamics intrinsic to the system and the time correlations set by the imposed timescale making the study of the nature of dynamic (multi)scaling, when such effects are at play, nontrivial.

One of the more natural and ubiquitous examples of turbulence with an imposed global timescale is that of rotating turbulence [33–36], observed in geophysical phenomena [37] including oceanic and atmospheric flows [38], astrophysical phenomena [39], and many engineering applications. When the Coriolis force dominates over the nonlinear term, strongly rotating, but mildly turbulent, three-dimensional flows tend to become two dimensional, consistent with the Taylor-Proudman theorem [35,40]. However, when the flow becomes turbulent, the nonlinear effects can no longer be ignored [20,41–46]. In fact, the nonlinear interactions among the inertial waves play an important role in developing the quasi-two-dimensional behavior of rotating turbulence [47–53].

In such rotating turbulent flows, the addition of a global rotation rate Ω through the Coriolis force sets a unique timescale $1/\Omega$. At the level of statics, we know [54] that this timescale leads to a characteristic length scale in the problem: the Zeman scale $\ell_\Omega = \sqrt{\varepsilon/\Omega^3}$, where ε is the mean kinetic energy dissipation. The role of this global rotation, via the

*skrathor@iitk.ac.in

†sagarc@iitk.ac.in

‡samriddhisankarray@gmail.com

Zeman scale, in determining the equal-time statistics of three-dimensional rotating turbulence has been extensively studied. In particular, we know that, unlike homogeneous and isotropic turbulence, in the limit of large Reynolds numbers, when $L \gg \ell_\Omega \gg \eta$, the equal-time (longitudinal) structure functions of the (projected) velocity increments $\delta u(r) = [\mathbf{u}(\mathbf{x} + \mathbf{r}) - \mathbf{u}(\mathbf{x})] \cdot \hat{\mathbf{r}}$ in the inertial range $L \gg r \gg \eta$ show a dual scaling; $\hat{\mathbf{r}}$ is the unit vector along the separation vector \mathbf{r} .

More precisely, defining the p th-order equal-time structure function $S_p(r) = \langle |\delta u(r)|^p \rangle$, the equal-time exponents are extracted via the power law $S_p(r) = r^{\zeta_p}$ in the inertial range. The rotation-induced Zeman scale results in two different classes of exponents: Theoretical estimates suggest that for the rotation-dominated larger scales $L \gg r \gg \ell_\Omega$, the exponents $\zeta_p = p/2$; however, at smaller scales $\ell_\Omega \gg r \gg \eta$, which are less sensitive to the Coriolis effects, $\zeta_p = p/3$, as is the case for fully developed three-dimensional turbulence [18–21]. A consequence of this is that kinetic energy spectrum $E(k)$ also displays dual scaling [54–57]: $E(k) = k^{-2}$ and $E(k) = k^{-5/3}$ for wave numbers smaller and larger, respectively, than the Zeman wave number $k_\Omega = 1/\ell_\Omega$. This dual scaling of the energy spectra is seen remarkably well in shell models, such as the one we use here, as shown in Fig. 1 of Ref. [21]. Of course, measurements suggest strong intermittency corrections to this simple dimensional form. Thus, in rotating turbulence, just like in homogeneous, isotropic turbulence, there exists multiscaling at the level of equal-time statistics.

However, is there a similar multiscaling for the dynamic correlators in such systems? This remains a somewhat open question because while different aspects of Lagrangian turbulence of rotating flows have been studied [49,58–61], studies of dynamic correlators are sparse [62,63]. Furthermore, these studies [62,63] use an Eulerian approach to measure the second-order dynamic correlation function which, as we know from insights developed in nonrotating turbulence [26], can lead to an oversimplification and mask an underlying multiscaling as we illustrate below.

In the much simpler nonrotating, homogeneous, isotropic turbulent flow, a naive calculation of dynamic scaling within the Eulerian framework, in a manner similar to what is done for equal-time structure functions, yields a trivial dynamic exponent of unity because the sweeping effect dominates and thus linearly couples the temporal and spatial scales. Indeed, this sweeping effect leads to the simpler dynamic exponents for the Eulerian time-dependent correlation functions in rotating turbulence as well, as reported by Favier *et al.* [62].

Thus, unlike for equal-time structure functions, special care must be taken which eliminates this sweeping effect in order to obtain nontrivial dynamic (multi)scaling exponents. This can be done through the Lagrangian or the quasi-Lagrangian framework [25–28,32,64–66]. While the former allows us to measure the structure functions of temporal velocity increments $\delta \mathbf{u}(\tau) = \mathbf{u}(t + \tau) - \mathbf{u}(t)$, the latter is especially useful as it allows us to obtain time-dependent structure functions for velocity increments and hence, in the limiting case, recovers the (Eulerian) equal-time structure functions [32,67], as we now show. The quasi-Lagrangian velocity field

$$\mathbf{v}(\mathbf{r}_0, t_0 | \mathbf{x}, t_0 + t) \equiv \mathbf{u}(\mathbf{x} + \mathbf{R}_L(\mathbf{r}_0, t_0 | t_0 + t), t_0 + t) \quad (1)$$

is measured along the Lagrangian trajectory $\mathbf{R}_L(\mathbf{r}_0, t_0 | t_0 + t)$ of a fluid particle starting at (\mathbf{r}_0, t_0) . This allows us to define the (quasi-Lagrangian) velocity increments $\delta v(r, t) = [\mathbf{v}(\mathbf{r}_0, t_0 | \mathbf{x} + \mathbf{r}, t_0 + t) - \mathbf{v}(\mathbf{r}_0, t_0 | \mathbf{x}, t_0 + t)] \cdot \hat{\mathbf{r}}$ and thence the time-dependent structure function $\mathcal{F}_p(r, t_1, \dots, t_p) \equiv \langle \delta v(r, t_1) \delta v(r, t_2) \cdots \delta v(r, t_p) \rangle$. By setting $t_1 = t_2 = \cdots = t_p = t$, the quasi-Lagrangian time-dependent structure function is written simply as $\mathcal{F}_p(r, t)$, with the obvious identity $\mathcal{F}_p(r, t = 0) \equiv S_p(r)$.

The quasi-Lagrangian structure function also lends itself to an adaptation of the Frisch-Parisi multifractal formalism [3,30] for the equal-time structure function. Assuming a multifractal description of rotating turbulence, the velocity field ought to possess a range of (universal) scaling exponents $h \in \mathcal{I} \equiv (h_{\min}, h_{\max})$, each of which corresponds to a fractal set Σ_h of dimension $\mathcal{D}(h)$. This allows us to write down the velocity increments $\delta u(\mathbf{x}, r)/u_L \propto (r/L)^h$, where u_L is the velocity associated with the large length scale of the flow. Given the multifractal description, for individual increments it is important to keep track of the point \mathbf{x} at which the increments are taken because the increment picks up different scaling exponents h for every $\mathbf{x} \in \Sigma_h$.

Such a prescription allows us to define the equal-time structure function in terms of the scaling exponents h and the measure $d\mu(h)$, which gives the weight of the contributing fractal sets:

$$S_p(r) \propto u_L^p \int_{\mathcal{I}} d\mu(h) \left(\frac{r}{L}\right)^{ph+3-\mathcal{D}(h)}. \quad (2)$$

Formally, the measured scaling exponents ζ_p are then extracted through a saddle-point calculation.

We now extend the equal-time formalism for time-dependent structure functions

$$\mathcal{F}_p(r, t) \propto u_L^p \int_{\mathcal{I}} d\mu(h) \left(\frac{r}{L}\right)^{ph+3-\mathcal{D}(h)} \mathcal{G}^{p,h} \left(\frac{t}{\tau_{p,h,\Omega}(r)} \right), \quad (3)$$

where $\tau_{p,h,\Omega}(r)$ is the characteristic scale-dependent timescale of the flow. The scaling function $\mathcal{G}^{p,h}$ is unity at $t = 0$ and its integral is assumed to exist to allow us to define the integral timescale:

$$\mathcal{T}_p^I(r) = \left[\frac{1}{S_p(r)} \int_0^\infty \mathcal{F}_p(r, t) dt \right] \sim r^{\zeta_p}. \quad (4)$$

In order to proceed further and calculate the dynamic exponent ζ_p , we make reasonable assumptions about the timescale $\tau_{p,h,\Omega}$. The phenomenology of rotating turbulence suggests that in the rotation-dominated regime $L \gg r \gg \ell_\Omega$, to leading order, the timescale is set by the rotation rate Ω and hence $\tau_{p,h,\Omega} \propto 1/\Omega$. On the other side of the Zeman scale $\ell_\Omega \gg r \gg \eta$ however, we expect $\tau_{p,h,\Omega} \equiv \tau_{p,h} \propto r^{1-h}$, consistent with the ideas of homogeneous and isotropic turbulence.

By using standard tools to evaluate the integral in Eq. (4), we eventually obtain (see, e.g., Refs. [26,32])

$$\zeta_p \sim \begin{cases} 1 + (\zeta_{p-1} - \zeta_p), & \ell_\Omega \gg r \gg \eta \\ 0, & L \gg r \gg \ell_\Omega. \end{cases} \quad (5)$$

Furthermore, the same analysis suggests that for $L \gg r \gg \ell_\Omega$, the integral timescale $\mathcal{T}_p^I(r) \propto 1/\Omega$. Indeed, this form is perhaps not entirely surprising given the scale-independent form of $\tau_{p,h,\Omega}$.

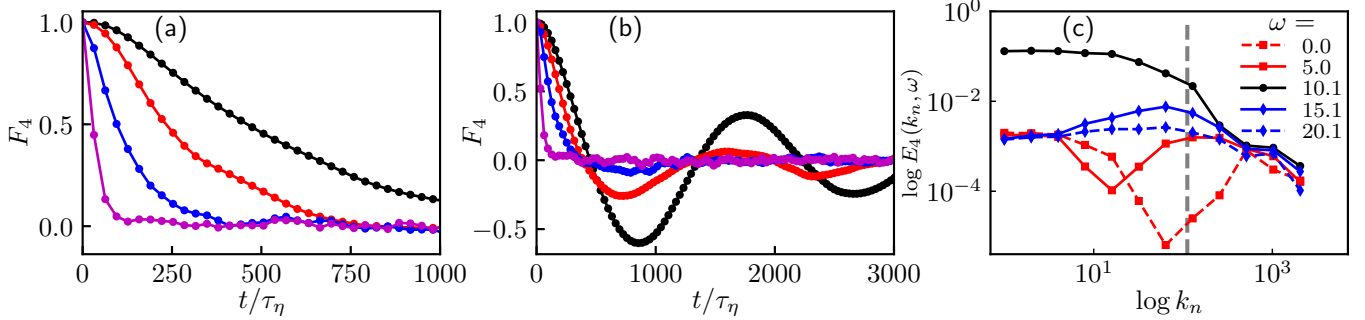


FIG. 1. Representative plots for the evolution of the normalized time-dependent fourth-order structure function $F_4(k_n, t)$ versus time, which is normalized by the Kolmogorov timescale τ_η for (a) $\text{Ro} = 0.161$ and (b) $\text{Ro} = 0.043$. The black, red, blue, and magenta lines correspond to $n = 11, 12, 14$, and 16 , respectively. (c) Plot of the relative spectral energy density $E_4(k_n, \omega)$ of $F_4(k_n, t)$ for $\text{Ro} = 0.043$ versus k_n for different harmonics ω ; the vertical dashed line represents the Zeman wave number.

Our predictions suggest that in rotating turbulence, the time-dependent structure functions also show dual scaling consistent with what we know from equal-time measurements. Indeed, the bridge relation connecting the integral-timescale-based dynamic exponent z_p for scales where turbulent fluctuations swamp the effect of rotation is identical to what happens in three-dimensional turbulent flows [26]. On the other hand, the dynamic structure functions are scale independent ($z_p = 0$) as soon as rotation is dominant. (It is perhaps useful to keep in mind that although to leading order our analysis shows that the integral timescale in the rotation-dominated regime is scale independent, the structure functions themselves are not, as we show below.)

Are our results surprising? The surprise and apparent contradiction arises when we examine the dynamics in terms of local turnover timescales of the flow $\mathcal{T}^{\text{local}}(r) \sim r/\delta u(r)$. For scales smaller than the Zeman scale by using $\delta u(r) \sim r^{1/3}$, we obtain the local p -independent dynamic exponent $z^{\text{local}} = 2/3$. This exponent is exactly the same as what we obtain from Eq. (5) in the absence of intermittency correction, i.e., $\zeta_p = p/3$. However, for scales larger than ℓ_Ω , a similar analysis yields $z^{\text{local}} = 1/2$ since $E(k) \sim k^{-2}$. This result is in sharp contradiction with the exponent $z_p = 0$ as obtained above (5) but also crucially suggests that in the rotation-dominant regime, the dynamic structure function is scale dependent.

This begs the question of which of these two approaches is correct and how is this contradiction resolved. Indeed, how valid are our theoretical predictions (5) when confronted with data from simulations?

While formally quasi-Lagrangian structures are well defined, measurements from direct numerical simulations of the three-dimensional Navier-Stokes equation are still a challenge [16,29]. Fortunately, this problem of circumventing sweeping through a quasi-Lagrangian description was solved [26] by adopting a shell model approach. Indeed, by construction, shell models are dynamical systems for (complex) variables which resemble velocity increments and sweeping is eliminated by restricting the coupling between modes which are only nearest or next-nearest neighbors. Remarkably, such a dynamical system approach to turbulence [3,6,68–70] does capture the essential multifractal and cascade processes of fully developed turbulence as recognized since the pioneering works of Obukhov [71], Desnyansky and Novikov

[72], Gledzer [73], and Ohkitani and Yamada [74] and then generalised to several other single and multiphase flows [9,13,16,27,75–87]. Moreover, shell models, although structurally isotropic, reproduce and predict many properties of the rotating turbulence, e.g., two-dimensionalization, the dual scaling of energy spectrum, and the scaling of equal-time structure functions [21,56,88].

Thus, given the question at hand, it is natural for us to approach this problem with a shell model for rotating turbulence. Such models are constructed on a logarithmically spaced lattice of wave numbers $k_n = k_0 \lambda^n$; we use the conventional choices of $k_0 = \frac{1}{16}$ and $\lambda = 2$ in our study. Associated with each shell n is a complex variable u_n which mimics velocity increments over a scale $k_n \sim 1/r$ in the Navier-Stokes equation. By retaining only the nearest- and next-nearest-neighbor couplings in the nonlinear (convolution) term of the Navier-Stokes equation, the shell model equations are coupled ordinary differential equations

$$\frac{du_n}{dt} = -\nu k_n^2 u_n + f_n - i\Omega u_n + i[ak_{n+1}u_{n+2}u_{n+1} + bk_n u_{n+1}u_{n-1} + ck_{n-1}u_{n-1}u_{n-2}]^*, \quad (6)$$

with shell numbers running from 1 to N . The asterisk in the equation denotes a complex conjugation, $i \equiv \sqrt{-1}$, and, as noted before, the nonlinear couplings are limited, ensuring the absence of direct coupling of large and small scales effectively eliminating sweeping effects. The shell model, in the absence of viscosity ($\nu = 0$) and external forcing $f_n = 0$, conserves energy, helicity, and phase space through a proper choice of the (real) coefficients a , b , and c ; we use, as is common, $a = 1$, $b = -\frac{1}{2}$, and $c = -\frac{1}{2}$ [89,90].

We characterize rotating turbulent flows not only by the (large-scale) Reynolds number $\text{Re} \equiv U_{\text{rms}}/k_0\nu$, where the root-mean-square velocity $U_{\text{rms}} = (\sum_n |u_n|^2)^{1/2}$ [69], but also by the Rossby number $\text{Ro} \equiv U_{\text{rms}}k_0/\Omega$, which is a measure of the relative strength of the nonlinearity to the Coriolis force and the Zeman wave number $k_\Omega = \sqrt{\Omega^3/\varepsilon}$. We use in our simulations Reynolds number $\text{Re} \sim 10^9$ and $\text{Ro} = \infty$ ($\Omega = 0; k_\Omega = 0$), 0.809 ($\Omega = 0.1; k_\Omega = 0.3$), 0.232 ($\Omega = 0.5; k_\Omega = 3.5$), 0.161 ($\Omega = 1.0; k_\Omega = 10.0$), and 0.043 ($\Omega = 5.0; k_\Omega = 111.8$).

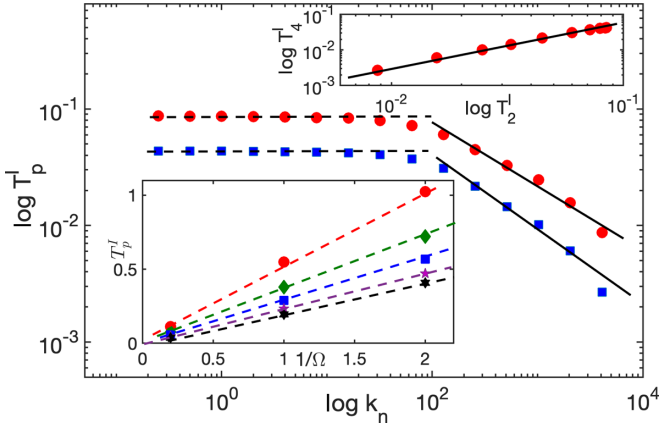


FIG. 2. A log-log (base 10) plot of the integral time $T_p^I(k_n)$ versus k_n for $p = 2$ (red circles) and $p = 4$ (blue squares) for $Ro = 0.043$. The dashed horizontal lines are best fits ($z_p = 0$) for wave numbers lower than the Zeman wave number and the thick black lines are the best fits in the inertial range not dominated by rotation ($z_p \neq 0$; see Table I). The lower inset shows a plot of T_p^I ($p = 2-6$, from the uppermost to the lowermost plot), for $k_n \lesssim k_\Omega$, vs $1/\Omega$ (except for $\Omega = 0.1$, where the plateau extends for just a few shells) for different values of p . The dashed lines are linear fits which show $T_p^I \propto 1/\Omega$, consistent with the theoretical prediction. The upper inset shows a plot of the fourth-order vs second-order integral timescales, which shows a convincing scaling with slope $z_4/z_2 \approx 1.09$, consistent with the exponent ratio obtained from the bridge relation.

From the statistically steady velocity field of the rotating turbulent flow [89], it is simple to define the shell model analog of the order- p , scale-dependent, quasi-Lagrangian normalized time-dependent structure function as

$$F_p(k_n, t) = \text{Re} \frac{\langle [u_n(t_0)u_n^*(t_0 + t)]^{p/2} \rangle}{\langle |u_n(t_0)|^p \rangle}, \quad (7)$$

where Re denotes the real part of the function and the angular brackets denote an average over different time origins t_0 . We choose integer values of p between 1 and 6 in this study.

In Fig. 1(a) we show representative plots of the fourth-order time-dependent structure function $F_4(k_n, t)$ for $Ro = 0.161$ and different shell numbers which are all greater than the Zeman scale and hence much less influenced by the effects

of rotation. As one would expect, the correlations decay much faster for higher wave numbers than for lower wave numbers.

To present the effect of rotation clearly, we go to a lower value of the Rossby number (hence a higher value of the Zeman wave number). Figure 1(b) shows such a plot for $Ro = 0.043$ for the same wave numbers as in Fig. 1(a). However, for such a low value of Ro , shell numbers $n = 11$ and 12 , corresponding to wave numbers close to the Zeman scale, are clearly affected by the Coriolis force. This is clearly seen in the conspicuous oscillatory profile of the structure function.

These oscillations arise, as already shown through the direct numerical simulations of Eulerian time-dependent correlators in Refs. [62,63], at rotation-dominated scales $k \lesssim k_\Omega$ because of the presence of the Coriolis term. Indeed, the formal solution of Eq. (6) ought to have a dominant harmonic $\sim \exp(-i\Omega t)$, in addition to the contributions of viscosity and the nonlinearity; this oscillatory factor of course becomes vanishingly small when $k_n \gg k_\Omega$. Consequently, for $k_n \lesssim k_\Omega$ [Fig. 1(b), $n = 11$ and 12], the time-dependent structure functions $F_p(k_n, t)$ have an oscillatory profile with a dominant harmonic of angular frequency $\sim p\Omega t/2$. For wave numbers $k_n \gg k_\Omega$, the nonlinearity of the dynamical systems ensures a mixing of the harmonics of different scales results in several sub- and superharmonics in the system eventually eliminating the clear oscillatory profile seen for $k_n \lesssim k_\Omega$.

This picture is easily validated, through a Fourier decomposition, from measurements of the spectral relative energy content $E_p(k_n, \omega) \equiv |\hat{F}_p(k_n, \omega)|^2 / \sum_n |\hat{F}_p(k_n, \omega)|^2$; here $\hat{F}_p(k_n, \omega)$ is the Fourier transform of $F_p(k_n, t)$. Figure 1(c) illustrates such an analysis, for $p = 4$ and $R = 0.043$ corresponding to the structure functions in Fig. 1(b), which clearly shows that while all the energy is maximally contained, for $k_n \lesssim k_\Omega$, in the $\omega \sim 10$ (corresponding to $Ro = 0.043$) mode, at wave numbers $k_n \gg k_\Omega$ the energy is distributed more uniformly among the other harmonics that we calculate.

From the time-dependent structure functions of the sort shown in Figs. 1(a) and 1(b), we define the p th-order shell-model analog of the integral timescale $T_p^I(k_n) \equiv \int_0^\infty F_p(k_n, t) dt$. In practice (to avoid contamination from statistical noise at long times [26]), the upper limit of the integral is restricted to times when $F_p(k_n, t)$ has reached a value of 0.6 and we have checked that our results are insensitive if this limit is varied between 0.4 and 0.8.

TABLE I. Summary, for $k_n \gg k_\Omega$, of our results for the dynamic exponents z_p (column 3) calculated through the bridge relations (5) from the equal-time exponents ζ_p obtained through ESS [91–93] (column 2) for different orders p (column 1). Columns 4–6 lists the dynamic exponents for different Rossby numbers obtained directly from our shell model simulations. (We note that the marginal increase in the error bars and mean exponents, while still being consistent with the theoretical prediction, as $Ro \rightarrow 0$ is likely due to the shrinking of the inertial range $k_n \gg k_\Omega$ as k_Ω becomes larger with decreasing Rossby numbers.)

| p | ζ_p | z_p [Eq. (5)] | z_p | | | |
|-----|-------------------|-------------------|-------------------|-------------------|-------------------|-----------------|
| | | | $Ro = 0.809$ | $Ro = 0.232$ | $Ro = 0.161$ | $Ro = 0.043$ |
| 1 | 0.379 ± 0.006 | 0.621 ± 0.006 | 0.63 ± 0.01 | 0.64 ± 0.02 | 0.65 ± 0.03 | 0.67 ± 0.07 |
| 2 | 0.707 ± 0.005 | 0.672 ± 0.008 | 0.673 ± 0.009 | 0.68 ± 0.01 | 0.68 ± 0.01 | 0.67 ± 0.06 |
| 3 | 1.0 | 0.707 ± 0.005 | 0.719 ± 0.009 | 0.703 ± 0.009 | 0.72 ± 0.01 | 0.73 ± 0.04 |
| 4 | 1.267 ± 0.007 | 0.733 ± 0.007 | 0.72 ± 0.01 | 0.72 ± 0.01 | 0.746 ± 0.008 | 0.76 ± 0.02 |
| 5 | 1.51 ± 0.02 | 0.75 ± 0.02 | 0.72 ± 0.02 | 0.74 ± 0.01 | 0.761 ± 0.008 | 0.79 ± 0.02 |
| 6 | 1.74 ± 0.03 | 0.77 ± 0.03 | 0.76 ± 0.02 | 0.75 ± 0.02 | 0.78 ± 0.01 | 0.80 ± 0.03 |

In Fig. 2 we show log-log plots of $T_2^I(k_n)$ and $T_4^I(k_n)$ vs k_n for $Ro = 0.043$. Clearly, for $k_n \lesssim k_\Omega$, the plateau in $T_p^I(k_n)$ leads to a dynamic exponent $z_p = 0$ as indicated by the dashed best-fit lines. In the lower inset, we plot the values of these plateau for different orders vs $1/\Omega$; the dashed line fit for each order shows clearly that the theoretical prediction from the multifractal analysis $T_p^I \propto 1/\Omega$, for $k_n \lesssim k_\Omega$, holds. However, for $k_n \gg k_\Omega$, the integral timescale seems to be clearly a power law with $z_p \neq 0$ which extends over a decade as shown by the black lines which best fit the data. From plots such as these we extract, through a least-squares fit, z_p (for different values of Ro) from 500 different measurements; in Table I we list the mean of these exponents and their standard deviations as error bars. To further illustrate the quality of the scaling range for higher wave numbers, in the upper inset we show a log-log plot of the fourth vs the second-order integral timescale in a manner reminiscent of the extended self-similarity (ESS) [91–93] technique used for equal-time measurements. This representation shows a clear scaling with the best-fit (black line) slope $z_4/z_2 \approx 1.09$, consistent with what one would obtain from the multifractal theory. While this ESS-like approach is convincing, we would advise caution in overinterpreting the role of such an extended self-similarity for dynamic exponents in the absence of a theory analogous to what is known for equal-time structure functions [91–93].

Comparing the different columns in Table I, it is clear that the bridge relations (5) are indeed satisfied for all Rossby numbers for wave numbers $k_n \gg k_\Omega$. Furthermore, in the rotation-dominated scales $k_n \lesssim k_\Omega$, we find (within error bars) $z_p = 0$, again consistent with our theoretical prediction (5).

In this paper we have addressed the issue of dynamic scaling in rotating turbulence by using the tools of the Frisch-Parisi multifractal formalism and then validated our predictions through detailed numerical simulations of a shell model which factors in the Coriolis force. By adopting a quasi-Lagrangian approach, our work complements earlier (Eulerian) studies [62,63] of time-dependent correlation func-

tions in such flows. We obtained a set of exponents (5) and associated bridge relations and found, unsurprisingly, for wave numbers larger than the Zeman scale, that even strongly rotating flows show dynamic multiscaling which is completely consistent with what has been known [26,28]. Surprisingly, for wave numbers which are dominated by the rotation, the relevant timescales are scale independent and thence $z_p = 0$, in sharp contrast to estimates from local timescale arguments. This is because at such scales rotation is the dominant mechanism when compared with those imposed by the nonlinear term. Hence, naively, one would expect that the dominant timescale here would be $\sim 1/\Omega$; the multifractal approach picks out this dominant timescale over all others. This is perhaps because at these scales a local turnover time approach fails to factor in the timescale imposed on the flow by rotation which dominates over the intrinsic (and local) timescales arising in the flow itself. Thus a comparison of the timescales which emerge from arguments based on the turnover time with those from the multifractal model showed a greater disparity at rotation-dominated scales than those which are not underlining the singular nature of the Coriolis force especially when it comes to dynamic correlators. Furthermore, curiously, the intermittency corrections seen in the equal-time measurements seem to be absent from the dynamics altogether. This is an example of a turbulent flow where such a decoupling of a fundamental feature of turbulence happens when we move from the statics to the dynamics and deserves more rigorous investigation in the future.

S.S.R. acknowledges the support from SERB-DST (India) through Projects No. MTR/2019/001553, No. STR/2021/000023, and No. CRG/2021/002766 and DAE, Government of India, through Projects No. 12-R&D-TFR-5.10-1100 and No. RTI4001. S.K.R. and S.C. gratefully acknowledge the support and the resources provided by PARAM Sanganak under the National Supercomputing Mission, Government of India at the Indian Institute of Technology, Kanpur.

-
- [1] A. S. Monin and A. M. Yaglom, *Statistical Fluid Mechanics*, edited by J. L. Lumley (MIT Press, Cambridge, 1971), Vol. 1.
 - [2] A. S. Monin and A. M. Yaglom, *Statistical Fluid Mechanics*, edited by J. L. Lumley (MIT Press, Cambridge, 1975), Vol. 2.
 - [3] U. Frisch, *Turbulence: The Legacy of A. N. Kolmogorov* (Cambridge University Press, Cambridge, 1995).
 - [4] A. N. Kolmogorov, Dokl. Akad. Nauk SSSR **30**, 301 (1941).
 - [5] A. N. Kolmogorov, Dokl. Akad. Nauk SSSR **32**, 16 (1941).
 - [6] M. H. Jensen, G. Paladin, and A. Vulpiani, *Phys. Rev. A* **43**, 798 (1991).
 - [7] K. R. Sreenivasan and R. A. Antonia, *Annu. Rev. Fluid Mech.* **29**, 435 (1997).
 - [8] R. H. Kraichnan, *Phys. Rev. Lett.* **72**, 1016 (1994).
 - [9] A. Wirth and L. Biferale, *Phys. Rev. E* **54**, 4982 (1996).
 - [10] Z. Warhaft, *Annu. Rev. Fluid Mech.* **32**, 203 (2000).
 - [11] M. K. Verma, *Phys. Rep.* **401**, 229 (2004).
 - [12] G. Sahoo, P. Perlekar, and R. Pandit, *New J. Phys.* **13**, 013036 (2011).
 - [13] D. Banerjee, S. S. Ray, G. Sahoo, and R. Pandit, *Phys. Rev. Lett.* **111**, 174501 (2013).
 - [14] G. Boffetta, A. Celani, S. Musacchio, and M. Vergassola, *Phys. Rev. E* **66**, 026304 (2002).
 - [15] Y.-K. Tsang, E. Ott, T. M. Antonsen, and P. N. Guzdar, *Phys. Rev. E* **71**, 066313 (2005).
 - [16] S. S. Ray, D. Mitra, P. Perlekar, and R. Pandit, *Phys. Rev. Lett.* **107**, 184503 (2011).
 - [17] G. Boffetta and R. E. Ecke, *Annu. Rev. Fluid Mech.* **44**, 427 (2012).
 - [18] W.-C. Müller and M. Thiele, *Europhys. Lett.* **77**, 34003 (2007).
 - [19] J. Seiwert, C. Morize, and F. Moisy, *Phys. Fluids* **20**, 071702 (2008).
 - [20] M. Thiele and W.-C. Müller, *J. Fluid Mech.* **637**, 425 (2009).
 - [21] S. K. Rathor, M. K. Sharma, S. S. Ray, and S. Chakraborty, *Phys. Fluids* **32**, 095104 (2020).

- [22] P. Chaikin and T. Lubensky, *Principles of Condensed Matter Physics* (Cambridge University Press, Cambridge, 1998).
- [23] R. Pandit, P. Perlekar, and S. S. Ray, *Pramana* **73**, 157 (2009).
- [24] P. C. Hohenberg and B. I. Halperin, *Rev. Mod. Phys.* **49**, 435 (1977).
- [25] D. Mitra and R. Pandit, *Physica A* **318**, 179 (2003).
- [26] D. Mitra and R. Pandit, *Phys. Rev. Lett.* **93**, 024501 (2004).
- [27] D. Mitra and R. Pandit, *Phys. Rev. Lett.* **95**, 144501 (2005).
- [28] S. S. Ray, D. Mitra, and R. Pandit, *New J. Phys.* **10**, 033003 (2008).
- [29] L. Biferale, E. Calzavarini, and F. Toschi, *Phys. Fluids* **23**, 085107 (2011).
- [30] U. Frisch and G. Parisi, in *Turbulence and Predictability in Geophysical Fluid Dynamics and Climate Dynamics*, edited by M. Ghil, R. Benzi, and G. Parisi (North-Holland, New York, 1985), pp. 84–87.
- [31] F. Hayot and C. Jayaprakash, *Phys. Rev. E* **57**, R4867 (1998).
- [32] V. S. L'vov, E. Podivilov, and I. Procaccia, *Phys. Rev. E* **55**, 7030 (1997).
- [33] Greenspan, *The Theory of Rotating Fluids* (Cambridge University Press, Cambridge, 1968).
- [34] A. Ibbetson and D. J. Tritton, *J. Fluid Mech.* **68**, 639 (1975).
- [35] P. A. Davidson, *Turbulence in Rotating, Stratified and Electrically Conducting Fluids* (Cambridge University Press, Cambridge, 2013).
- [36] F. S. Godeferd and F. Moisy, *Appl. Mech. Rev.* **67**, 030802 (2015).
- [37] J. Aurnou, M. Calkins, J. Cheng, K. Julien, E. King, D. Nieves, K. Soderlund, and S. Stellmach, *Phys. Earth Planet. In.* **246**, 52 (2015).
- [38] J. Y.-K. Cho, K. Menou, B. M. S. Hansen, and S. Seager, *Astrophys. J.* **675**, 817 (2008).
- [39] S. A. Barnes, *Astrophys. J.* **561**, 1095 (2001).
- [40] G. I. Taylor and H. Lamb, *Proc. R. Soc. London Ser. A* **93**, 99 (1917).
- [41] O. Métais, P. Bartello, E. Garnier, J. Riley, and M. Lesieur, *Dyn. Atmos. Oceans* **23**, 193 (1996).
- [42] L. M. Smith and F. Waleffe, *Phys. Fluids* **11**, 1608 (1999).
- [43] P. D. Mininni, A. Alexakis, and A. Pouquet, *Phys. Fluids* **21**, 015108 (2009).
- [44] E. Yarom, Y. Vardi, and E. Sharon, *Phys. Fluids* **25**, 085105 (2013).
- [45] M. K. Sharma, M. K. Verma, and S. Chakraborty, *Phys. Fluids* **30**, 115102 (2018).
- [46] M. K. Sharma, A. Kumar, M. K. Verma, and S. Chakraborty, *Phys. Fluids* **30**, 045103 (2018).
- [47] E. J. Hopfinger, F. K. Browand, and Y. Gagne, *J. Fluid Mech.* **125**, 505 (1982).
- [48] C. Cambon and L. Jacquin, *J. Fluid Mech.* **202**, 295 (1989).
- [49] L. Biferale, F. Bonaccorso, I. M. Mazzitelli, M. A. T. van Hinsberg, A. S. Lanotte, S. Musacchio, P. Perlekar, and F. Toschi, *Phys. Rev. X* **6**, 041036 (2016).
- [50] S. Galtier, *Phys. Rev. E* **68**, 015301(R) (2003).
- [51] C. Cambon, R. Rubinstein, and F. S. Godeferd, *New J. Phys.* **6**, 73 (2004).
- [52] G. P. Bewley, D. P. Lathrop, L. R. M. Maas, and K. R. Sreenivasan, *Phys. Fluids* **19**, 071701 (2007).
- [53] T. L. Reun, B. Favier, A. J. Barker, and M. L. Bars, *Phys. Rev. Lett.* **119**, 034502 (2017).
- [54] O. Zeman, *Phys. Fluids* **6**, 3221 (1994).
- [55] Y. Zhou, *Phys. Fluids* **7**, 2092 (1995).
- [56] S. Chakraborty, M. H. Jensen, and A. Sarkar, *Eur. Phys. J. B* **73**, 447 (2010).
- [57] D. Chakraborty and J. K. Bhattacharjee, *Phys. Rev. E* **76**, 031117 (2007).
- [58] C. Cambon, F. S. Godeferd, F. C. G. A. Nicolleau, and J. C. Vassilicos, *J. Fluid Mech.* **499**, 231 (2004).
- [59] L. D. Castello and H. J. H. Clercx, *J. Phys.: Conf. Ser.* **318**, 052028 (2011).
- [60] E. Yarom, A. Salhov, and E. Sharon, *Phys. Rev. Fluids* **2**, 122601(R) (2017).
- [61] P. Maity, R. Govindarajan, and S. S. Ray, *Phys. Rev. E* **100**, 043110 (2019).
- [62] B. Favier, F. S. Godeferd, and C. Cambon, *Phys. Fluids* **22**, 015101 (2010).
- [63] P. C. di Leoni, P. J. Cobelli, P. D. Mininni, P. Dmitruk, and W. H. Matthaeus, *Phys. Fluids* **26**, 035106 (2014).
- [64] L. Biferale, G. Boffetta, A. Celani, and F. Toschi, *Physica D* **127**, 187 (1999).
- [65] Y. Kaneda, T. Ishihara, and K. Gotoh, *Phys. Fluids* **11**, 2154 (1999).
- [66] R. Pandit, S. S. Ray, and D. Mitra, *Eur. Phys. J. B* **64**, 463 (2008).
- [67] V. I. Belinicher and V. S. L'vov, *Sov. Phys. JETP* **66**, 303 (1987).
- [68] M. H. Jensen, *Phys. Rev. Lett.* **83**, 76 (1999).
- [69] L. Biferale, *Annu. Rev. Fluid Mech.* **35**, 441 (2003).
- [70] T. Bohr, M. H. Jensen, G. Paladin, and A. Vulpiani, *Dynamical Systems Approach to Turbulence* (Cambridge University Press, Cambridge, 1998).
- [71] A. M. Obukhov, *Atmos. Ocean. Phys.* **10**, 127 (1974).
- [72] V. N. Desnyansky and E. A. Novikov, *Prikl. Mat. Mekh.* **38**, 507 (1974).
- [73] E. B. Gledzer, *Sov. Phys. Dokl. SSSR* **18**, 216 (1973).
- [74] K. Ohkitani and M. Yamada, *Prog. Theor. Phys.* **81**, 32941 (1982).
- [75] E. Aurell, G. Boffetta, A. Crisanti, P. Frick, G. Paladin, and A. Vulpiani, *Phys. Rev. E* **50**, 4705 (1994).
- [76] P. Giuliani, M. H. Jensen, and V. Yakhot, *Phys. Rev. E* **65**, 036305 (2002).
- [77] P. Frick and D. Sokoloff, *Phys. Rev. E* **57**, 4155 (1998).
- [78] A. Basu, A. Sain, S. K. Dhar, and R. Pandit, *Phys. Rev. Lett.* **81**, 2687 (1998).
- [79] P. Giuliani and V. Carbone, *Europhys. Lett.* **43**, 527 (1998).
- [80] A. Brandenburg, K. Enqvist, and P. Olesen, *Phys. Rev. D* **54**, 1291 (1996).
- [81] D. Hori, M. Furukawa, S. Ohsaki, and Z. Yoshida, *J. Plasma Fusion Res.* **81**, 141 (2005).
- [82] S. Galtier, *Phys. Rev. E* **77**, 015302(R) (2008).
- [83] C. Kalelkar, R. Govindarajan, and R. Pandit, *Phys. Rev. E* **83**, 039903 (2005).
- [84] D. H. Wacks and C. F. Barenghi, *Phys. Rev. B* **84**, 184505 (2011).
- [85] L. Boué, V. L'vov, A. Pomyalov, and I. Procaccia, *Phys. Rev. B* **85**, 104502 (2012).

- [86] L. Boué, V. L'vov, A. Pomyalov, and I. Procaccia, *Phys. Rev. Lett.* **110**, 014502 (2013).
- [87] V. Shukla and R. Pandit, *Phys. Rev. E* **94**, 043101 (2016).
- [88] Y. Hattori, R. Rubinstein, and A. Ishizawa, *Phys. Rev. E* **70**, 046311 (2004).
- [89] See Supplemental Material at <http://link.aps.org/supplemental/10.1103/PhysRevE.105.L063102> for details on the numerical simulations, which includes Ref. [90].
- [90] L. Kadanoff, D. Lohse, J. Wang, and R. Benzi, *Phys. Fluids* **7**, 617 (1995).
- [91] R. Benzi, S. Ciliberto, R. Tripicciono, C. Baudet, F. Massaioli, and S. Succi, *Phys. Rev. E* **48**, R29 (1993).
- [92] S. Chakraborty, U. Frisch, and S. S. Ray, *J. Fluid Mech.* **649**, 275 (2010).
- [93] S. Chakraborty, U. Frisch, W. Pauls, and S. S. Ray, *Phys. Rev. E* **85**, 015301(R) (2012).